

14. Akitt, J. W. & Elders, J. M. Multinuclear magnetic resonance studies of the hydrolysis of aluminium(III). Part 8. Base hydrolysis monitored at very high magnetic field. *J. Chem. Soc. Dalton Trans.* 1347–1355 (1988).

15. Sullivan, D. J., Nordin, J. P., Phillips, B. L. & Casey, W. H. The rates of water exchange in Al(III)-salicylate and Al(III)-sulfosalicylate complexes. *Geochim. Cosmochim. Acta* **63**, 1471–1480 (1999).

16. Furrer, G., Gfeller, M. & Wehrli, B. On the chemistry of the Keggin Al₁₃ polymer – kinetics of proton-promoted decomposition. *Geochim. Cosmochim. Acta* **63**, 3069–3076 (2000).

17. Nordin, J. P., Sullivan, D. J., Phillips, B. L. & Casey, W. H. An ¹⁷O NMR study of the exchange of water on AlOH(H₂O)²⁺ (aq). *Inorg. Chem.* **37**, 4760–4763 (1998).

18. Thompson, A. R., Kunwar, A. C., Gutowsky, H. S. & Oldfield, E. Oxygen-17 and aluminum-27 nuclear magnetic resonance spectroscopic investigations of aluminum(III) hydrolysis products. *J. Chem. Soc. Dalton Trans.* 2317–2322 (1987).

19. Helm, L., Elding, L. I. & Merbach, A. E. Activation parameters and mechanism for water exchange of tetraaquaplatinum(II) studied by high-pressure oxygen-17 NMR spectroscopy. *Inorg. Chem.* **24**, 1719–1721 (1985).

20. Merbach, A. E. Use of high pressure kinetic studies in determining inorganic substitution mechanisms. *Pure Appl. Chem.* **59**, 161–172 (1987).

21. Parker, W. O'N. Jr, Millini, R. & Kiricsi, I. Metal substitution in Keggin-type tridecameric aluminum-oxo-hydroxo clusters. *Inorg. Chem.* **36**, 571–575 (1997).

22. Lee, M. A., Winter, N. W. & Casey, W. H. Investigation of the ligand exchange reaction for the aqueous Be²⁺ ion. *J. Phys. Chem.* **98**, 8641–8647 (1994).

23. Xiao, Y. T. & Lasaga, A. C. Ab initio quantum mechanical studies of the kinetics and mechanisms of silicate dissolution-H⁺ (H₃O⁺) catalysis. *Geochim. Cosmochim. Acta* **58**, 379–5400 (1994).

24. Kubicki, J. D., Blake, G. A. & Apitz, S. E. Molecular orbital calculations for modeling acetate-aluminosilicate adsorption and dissolution reactions. *Geochim. Cosmochim. Acta* **61**, 1031–1046 (1997).

25. Bradley, S. M., Kydd, R. A. & Howe, R. F. The structure of Al-gels formed through base hydrolysis of Al³⁺ aqueous solutions. *J. Colloid Interface Sci.* **159**, 405–412 (1993).

26. Fu, G., Nazar, L. F. & Bain, A. D. Aging processes of alumina sol-gels: Characterization of new aluminum polyoxocations by ²⁷Al NMR spectroscopy. *Chem. Mater.* **3**, 602–610 (1991).

Acknowledgements

We thank J. Nordin, S. Nordin, S. Crawford and D. Sullivan for help in the early stages of this work. This work was supported by the US NSF and the W.M. Keck Solid State NMR Laboratory at UC Davis.

Correspondence and requests for materials should be addressed to W.H.C. (e-mail: whcasey@ucdavis.edu).

Evidence that humans evolved from a knuckle-walking ancestor

Brian G. Richmond & David S. Strait

Department of Anthropology, The George Washington University, 2110 G Street, NW, Washington, DC 20052, USA

Bipedalism has traditionally been regarded as the fundamental adaptation that sets hominids apart from other primates. Fossil evidence demonstrates that by 4.1 million years ago¹, and perhaps earlier², hominids exhibited adaptations to bipedal walking. At present, however, the fossil record offers little information about the origin of bipedalism, and despite nearly a century of research on existing fossils and comparative anatomy, there is still no consensus concerning the mode of locomotion that preceded bipedalism^{3–10}. Here we present evidence that fossils attributed to *Australopithecus anamensis* (KNM-ER 20419)¹¹ and *A. afarensis* (AL 288-1)¹² retain specialized wrist morphology associated with knuckle-walking. This distal radial morphology differs from that of later hominids and non-knuckle-walking anthropoid primates, suggesting that knuckle-walking is a derived feature of the African ape and human clade. This removes key morphological evidence for a *Pan–Gorilla* clade, and suggests that bipedal hominids evolved from a knuckle-walking ancestor that was already partly terrestrial.

During knuckle-walking, chimpanzees and gorillas flex the tips of their fingers and bear their weight on the dorsal surface of their middle phalanges (Fig. 1), permitting them to use their hands for terrestrial locomotion while retaining long fingers for climbing

trees. Cineradiographic experiments show that during the middle and late propulsive phases of knuckle-walking, the carpus and metacarpus are slightly extended relative to the radius, and the proximal carpal joint remains static throughout the propulsive movement¹³. These observations indicate that the wrist is held in a stable, locked position during the support phase of knuckle-walking.

The mechanism by which the wrist locks into place consists of several components. The distal radius of African apes exhibits a distally projecting dorsal margin that gives the joint surface a volar tilt (Fig. 1)^{13,14}. Along this dorsal margin, a distally facing notch accommodates a corresponding concavity on the dorsal surface of the scaphoid (Fig. 1). During wrist extension, the spherical, convex portion of the scaphoid's proximal articular surface rotates until the concave portion engages the notch in a close-packed position¹³ (Fig. 1). This locking mechanism stabilizes the radiocarpal joint by limiting wrist extension during the support phase of knuckle-walking. This mechanism is corroborated by data on passive manipulation in which wrist extension is significantly more restricted in *Pan* and *Gorilla* than in *Pongo* and *Hylobates*^{13,15}. Furthermore, chimpanzees do not consistently recruit the major flexor muscles of the wrist during the support phase of knuckle-walking, suggesting that a passive mechanism exists for limiting extension¹⁶.

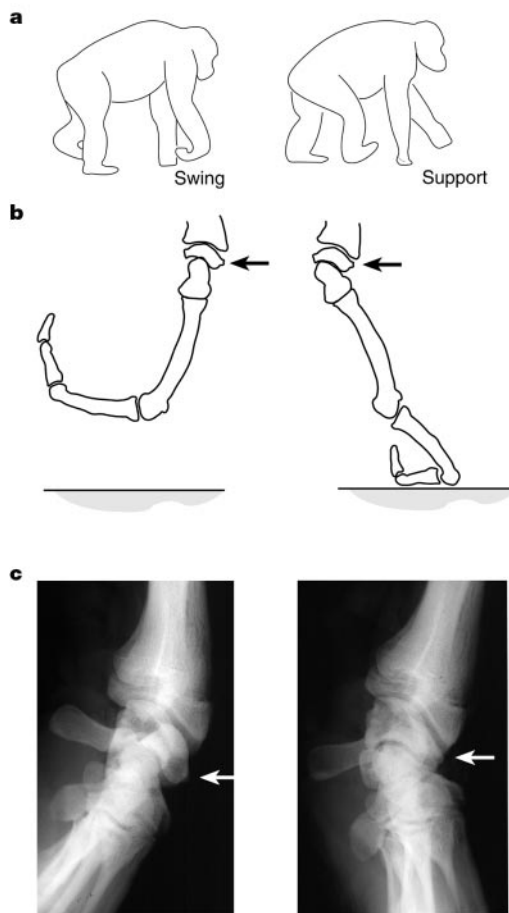


Figure 1 The wrist joint during the swing phase (left column) and support phase (right column) of knuckle-walking. Arrows in **b** and **c** denote the dorsal tip of the scaphoid. **a**, Outline of a chimpanzee during knuckle-walking. **b**, Schematic parasagittal slice of the hand of *Pan troglodytes* along the third ray. The slight concavity on the scaphoid accommodates a convexity on the distal radius. This convexity, the scaphoid notch, lies along the margin of a distally projecting dorsal ridge on the radius. **c**, Radiograph in mediolateral view of the wrist of *P. troglodytes*. Note the close-packed position in the extended wrist (right).

Wrist joint function during knuckle-walking differs from that of other modes of anthropoid pronograde quadrupedalism. Above-branch quadrupedalism in non-hominoid anthropoids typically involves more extended wrist postures along with palmigrady and less extended limbs^{17,18}. Two of the most adept anthropoid terrestrial quadrupeds differ from one another and from knuckle-walkers. Patas monkeys extend their wrists considerably during the late support phase and push-off of terrestrial locomotion¹⁸. In contrast, baboons maintain their wrists near the neutral position when locomoting on the ground, but employ more extended wrist postures while travelling on a branch¹⁷. Thus, wrist function during knuckle-walking seems to be unique compared with other forms of anthropoid quadrupedalism.

Building on published experimental studies^{13,14}, we identify four skeletal features of the distal radius as components of a morphological complex involved in stabilizing the wrist in extension during knuckle-walking. They are (1) the distal projection of the dorsal ridge, (2) the orientation of the scaphoid notch, (3) the size of the scaphoid notch, and (4) the relative orientations of the lunate and scaphoid articular surfaces (Fig. 2a). The distal projection of the dorsal ridge limits extension and might resist shearing forces, and the dorsal position of the notch for the scaphoid ensures that the

radius close-packs with the scaphoid in extension. A relatively large scaphoid notch reduces stress during weight support by increasing the area over which joint forces are distributed. In the radio-ulnar plane, the scaphoid and lunate articular surfaces of the African apes and non-hominoid anthropoids are roughly co-planar and face distomedially, presumably to resist stresses in that plane. In contrast, these surfaces are angled relative to each other in Asian apes, and might contribute to a ball-and-socket mechanism¹³.

A canonical variates analysis (Fig. 2b) based on the distal projection index, scaphoid notch angle, notch size index and scaphoid–lunate facet angle demonstrates that all extant taxa differ significantly from one another ($P < 0.001$ for all pairwise contrasts except *Papio*–*Erythrocebus*, $P < 0.015$). Notch size index and interfacet angle are the most influential variables along canonical axis 1, and the distal projection index dominates canonical axis 2. The Miocene hominoid *Proconsul heseloni* resembles extant howler monkeys, suggesting that the primitive hominoid condition is similar to that of a generalized anthropoid. The knuckle-walking African apes (*Pan* and *Gorilla*) are distinguished in the analysis by a combination of features, including a very prominent distally projecting dorsal ridge, a more dorsally oriented scaphoid notch, and a scaphoid notch and scaphoid–lunate angle that are small compared with those of other anthropoid quadrupeds but larger than those of Asian apes (Fig. 3). A UPGMA clustering diagram of the multivariate Mahalanobis D^2 distances illustrates the similarity between the radii of *A. anamensis* and *A. afarensis* and those of the knuckle-walking African apes (Fig. 2c), indicating that these hominids retain the derived wrist morphology of knuckle-walkers. Thus, the distally projecting dorsal ridge (Fig. 3) and distinct, dorsolaterally oriented scaphoid notch found in radii attributed to *A. anamensis* and *A. afarensis* indicate that wrist extension was limited in these hominids as in knuckle-walkers. The radius attributed to *Paranthropus robustus* is most similar to humans but is somewhat intermediate, and the radius of *A. africanus* is remarkably human-like (Figs 2b, 2c, 3). The sampling limitations of the fossil record do not allow us to assess the significance of variation between hominid species (except perhaps for the substantial difference between *A. africanus* and *A. anamensis/A. afarensis*). However, the hominids sort temporally such that the earliest fossils are the most African ape-like, and the later fossils more closely resemble modern humans, a pattern consistent with the hypothesis presented here.

Previous studies¹⁹ have noted that early hominids lack other distinctive knuckle-walking features, such as pronounced dorsal metacarpal ridges, and dorsally expanded and widened articular surfaces of the metacarpal heads²⁰, that increase the stability and range of extension in metacarpophalangeal joints. However, because these features are not always present in extant knuckle-walkers²⁰, their absence in hominids does not rule out knuckle-walking ancestry. Rather, the absence of these features in early hominids, in conjunction with clearly derived morphological evidence for bipedalism^{1,12,19}, suggests to us that early hominids did not themselves practise knuckle-walking. The total morphological pattern is consistent with the suggestion that the knuckle-walking morphology in the wrists of *A. anamensis* and *A. afarensis* was retained from a knuckle-walking ancestor. These results support earlier interpretations^{5,10} that fusion of the os centrale with the scaphoid, one of the few derived morphological characteristics shared by African apes and humans, is an adaptation to resist weight-bearing stresses and improve the stability of the hand in terrestrial quadrupedalism. Other traits shared between African apes and humans, such as robust metacarpals and phalanges and long middle phalanges relative to proximal phalanges, might also be retained knuckle-walking adaptations²¹.

Our results indicate that the behavioural/morphological complex associated with knuckle-walking is a synapomorphy of the African ape and human clade. This removes key morphological evidence uniting chimpanzees with gorillas to the exclusion of humans²², and

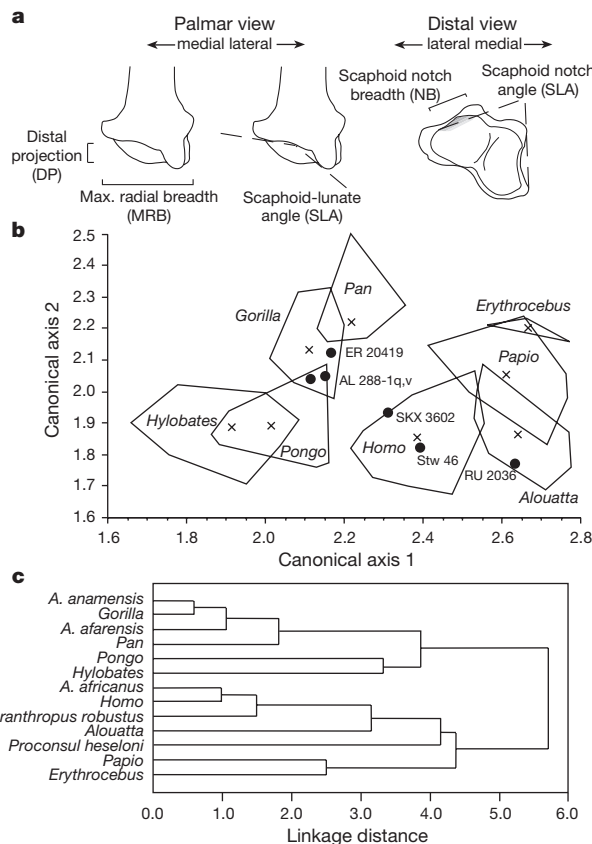


Figure 2 Measurements and canonical variates analysis (CVA) of the distal radius. **a**, Illustration of the measurements collected in palmar and distal views. **b**, Bivariate plot of canonical scores, based on CVA of four shape measurements (DPI, NSI, SNA and SLA). Observed ranges of extant taxa (polygons), taxon means (crosses) and fossil specimens (circles) are shown. The two measures for AL 288-1 come from the left and right radii of this individual. **c**, UPGMA clustering diagram of the Mahalanobis D^2 distances among groups in multidimensional space (not limited to the axes shown in **b**). Note in **b** and **c** that the earliest hominid taxa *A. anamensis* (KNM-ER 20419) and *A. afarensis* (AL 288-1) exhibit the derived knuckle-walking morphology, whereas *Paranthropus robustus* (SKX 3602) and especially *A. africanus* (Stw 46) more closely resemble modern humans.

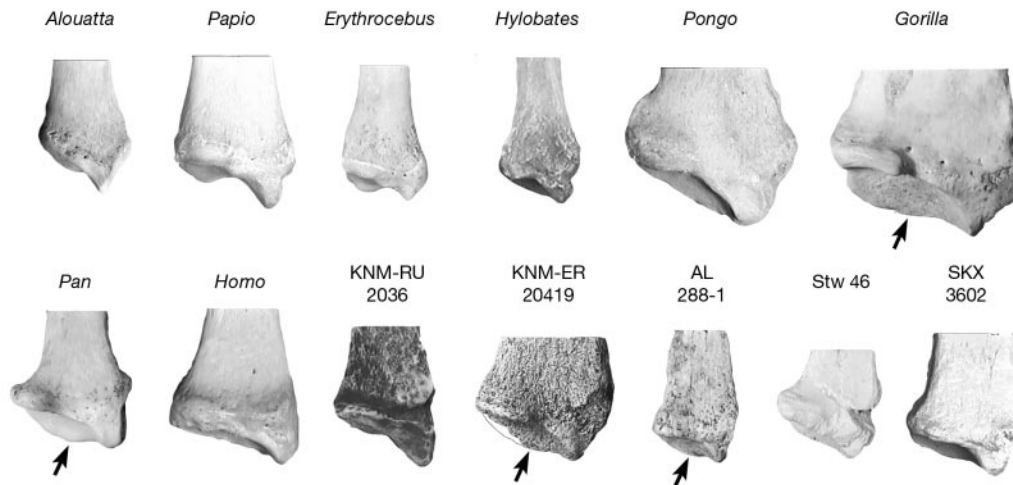


Figure 3 Palmar view of distal radii. All specimens except SKX 3602 (reversed) are left radii. The early hominid radii KNM-ER 20419 (*A. anamensis*) and AL 288-1 (*A. afarensis*) possess the distally projecting and medially extended dorsal ridge (arrows), and intermediate scaphoid notch size and scaphoid–lunate facet angle characteristic of the knuckle-walking African apes. In some specimens (for example, *Papio* and *Pan*), the

scaphoid notch is partly visible in palmar view as a concavity along the dorsal radial margin, just to the left of the styloid process. Note that the dorsal ridge in KNM-ER 20419 had been damaged along its medial extent and was reconstructed here for illustrative purposes. No measurements involved the reconstructed portion.

is consistent with other phylogenies based on morphological²³ and molecular²⁴ data that support a *Pan*–*Homo* clade. This further indicates that knuckle-walking did not originate independently in *Pan* and *Gorilla*. Thus, the differences observed between *Pan* and *Gorilla* in the growth of the ulnar side of the carpus²⁵ might be consequences of kinematic differences related to body size.

The retention of knuckle-walking morphology in the earliest hominids indicates that bipedalism evolved from an ancestor already adapted for terrestrial locomotion. However, early australopithecines also exhibit a number of postcranial traits related to arboreal locomotion, including a long radial neck, well-developed brachioradialis insertion¹¹, superiorly directed glenoid fossa, relatively long forelimbs and relatively long, curved fingers and toes¹⁹. Although there is some debate about the extent to which hominids such as *A. afarensis* continued to practise arboreality^{10,18,19}, the retention of arboreal morphology in early hominids suggests that at least their ancestors engaged in arboreal behaviours. Thus, the wealth of evidence illustrating the biomechanical similarities between climbing and bipedalism⁸ might still help to explain the morphological transition of an ape-like ancestor to an early biped. However, the present study does not support hypotheses in which the ancestor was completely committed to orthograde arboreality^{3,6,7}.

Pre-bipedal locomotion is probably best characterized as a repertoire consisting of terrestrial knuckle-walking, arboreal climbing and occasional suspensory activities⁹, not unlike that observed in chimpanzees today. This raises the question of why bipedalism would evolve from an ancestor already adapted to terrestrial locomotion, and is consistent with models relating the evolution of bipedalism to a change in feeding strategies²⁶ and novel non-locomotor uses of the hands^{4,9,27,28}. □

Methods

Measurements were collected on distal radii attributed to *Proconsul heseloni* (KNM-RU 2036)²⁹, *Australopithecus anamensis* (KNM-ER 20419)¹¹, *Australopithecus afarensis* (AL 288-1q.v)¹², *Australopithecus africanus* (Stw 46)³⁰ and *Paranthropus robustus* (SKX 3602)³⁰ to those of 19 *Hylobates* specimens (pooled *H. syndactylus*, *H. klossi*, *H. lar* and *H. concolor*), 13 *Pan troglodytes*, 17 *Gorilla gorilla*, 17 *Pongo pygmaeus*, 20 *Homo sapiens*, 19 *Papio anubis*, 3 *Erythrocebus patas* and 18 *Alouatta palliata*.

The distal projection (DP) of the dorsal ridge, maximum radial breadth (MRB) and scaphoid–lunate facet angle (SLA) were measured in palmar view, which was defined as the plane of the flattened anterior surface on the distal radial shaft just proximal to the epiphysis. In all anthropoids examined here this plane is roughly perpendicular to the

plane of the ulnar notch, which is oriented parasagittally during fully pronated and fully supinated hand postures, and approximates the plane in which the hand moves during wrist extension. Measurements were collected by digitizing high-resolution video images. In palmar view, each radius was positioned so that the midpoint of the palmar margin of the articular surface lay in the centre of the perpendicularly oriented video camera, and rotated until the lateral shaft margin lay superoinferiorly. Scaphoid notch breadth (NB) was defined as the length of the portion along the dorsal margin of the distal radial articular surface that is bevelled (indicated by shading in Fig. 2a) to articulate with the scaphoid. The scaphoid notch angle (SNA) was measured as the angle between the scaphoid and ulnar notches. The notch size index (NSI) was calculated as NB/MRB, and the distal projection index (DPI) as DP/MRB.

Received 10 August 1999; accepted 10 January 2000.

1. Leakey, M. G., Fiebel, C. S., McDougall, I. & Walker, A. C. New four-million-year-old hominid species from Kanapoi and Allia Bay, Kenya. *Nature* **376**, 565–571 (1995).
2. White, T. D., Suwa, G. & Asfaw, B. *Australopithecus ramidus*, a new species of early hominid from Aramis, Ethiopia. *Nature* **371**, 306–312 (1994).
3. Keith, A. Man's posture: its evolution and disorders. *Br. Med. J.* **1**, 451–454, 499–502, 545–548, 587–590, 624–626, 669–672 (1923).
4. Washburn, S. L. Behavior and the origin of man. *Proc. R. Anthropol. Inst. Gr. Br. Ireland* **3**, 21–27 (1967).
5. Marzke, M. W. Origin of the human hand. *Am. J. Phys. Anthropol.* **34**, 61–84 (1971).
6. Tuttle, R. H. Darwin's apes, dental apes, and the descent of man: normal science in evolutionary anthropology. *Curr. Anthropol.* **15**, 389–398 (1974).
7. Stern, J. T. Jr Before bipedality. *Yrbk Phys. Anthropol.* **19**, 59–68 (1975).
8. Fleagle, J. G. *et al.* Climbing: a biomechanical link with brachiation and bipedalism. *Symp. Zool. Soc. Lond.* **48**, 359–373 (1981).
9. Rose, M. D. in *Origine(s) de la Bipedie Chez les Hominides* (eds Coppens, Y. & Senut, B.) 37–48 (Centre National de la Recherche Scientifique, Paris, 1991).
10. Gebo, D. L. Climbing, brachiation, and terrestrial quadrupedalism: historical precursors of hominid bipedalism. *Am. J. Phys. Anthropol.* **101**, 55–92 (1996).
11. Heinrich, R. E., Rose, M. D., Leakey, R. E. & Walker, A. C. Hominid radius from the Middle Pliocene of Lake Turkana, Kenya. *Am. J. Phys. Anthropol.* **92**, 139–148 (1993).
12. Johanson, D. C. *et al.* Morphology of the Pliocene partial hominid skeleton (AL288-1) from the Hadar Formation, Ethiopia. *Am. J. Phys. Anthropol.* **57**, 403–451 (1982).
13. Jenkins, F. A. Jr & Fleagle, J. G. in *Primate Functional Morphology and Evolution* (ed. Tuttle, R. H.) 213–231 (Mouton, The Hague, 1975).
14. Tuttle, R. H. Knuckle-walking and the evolution of hominoid hands. *Am. J. Phys. Anthropol.* **26**, 171–206 (1967).
15. Tuttle, R. H. Quantitative and functional studies on the hands of the anthropoidea: I. The Hominoidea. *J. Morphol.* **128**, 309–363 (1969).
16. Susman, R. L. & Stern, J. T. Jr Telemetered electromyography of flexor digitorum profundus and flexor digitorum superficialis in *Pan troglodytes* and implications for interpretation of the O.H. 7 hand. *Am. J. Phys. Anthropol.* **50**, 565–574 (1979).
17. Schmitt, D. Forelimb mechanics as a function of substrate type during quadrupedalism in two anthropoid primates. *J. Hum. Evol.* **26**, 441–457 (1994).
18. Richmond, B. G. *Ontogeny and Biomechanics of Phalangeal Form in Primates*. Thesis, State Univ. New York at Stony Brook (1998).
19. Stern, J. T. Jr & Susman, R. L. The locomotor anatomy of *Australopithecus afarensis*. *Am. J. Phys. Anthropol.* **60**, 279–317 (1983).
20. Susman, R. L. Comparative and functional morphology of hominoid fingers. *Am. J. Phys. Anthropol.* **50**, 215–235 (1979).

21. Begun, D. R. Knuckle-walking ancestors. *Science* **259**, 294 (1993).
 22. Andrews, P. J. & Martin, L. B. Cladistic relationships of extant and fossil hominoids. *J. Hum. Evol.* **16**, 101–118 (1987).
 23. Begun, D. R. Miocene fossil hominids and the chimp-human clade. *Science* **257**, 1929–1933 (1992).
 24. Ruvolo, M. Molecular phylogeny of the hominoids: inferences from multiple independent DNA sequence data sets. *Mol. Biol. Evol.* **14**, 248–265 (1997).
 25. Dainton, M. & Macho, G. A. Did knuckle walking evolve twice? *J. Hum. Evol.* **36**, 171–194 (1999).
 26. Hunt, K. D. The postural feeding hypothesis: an ecological model for the origin of bipedalism. *S. Afr. J. Sci.* **9**, 77–90 (1996).
 27. Hewes, G. W. Food transport and the origin of hominid bipedalism. *Am. Anthropol.* **63**, 687–710 (1961).
 28. Lovejoy, C. O. The origin of man. *Science* **211**, 341–350 (1981).
 29. Napier, J. R. & Davis, P. The forelimb skeleton and associated remains of *Proconsul africanus*. *Foss. Mamm. Afr.* **16**, 1–70 (1959).
 30. Grine, F. E. & Susman, R. L. Radius of *Paranthropus robustus* from Member 1, Swartkrans Formation, South Africa. *Am. J. Phys. Anthropol.* **84**, 229–248 (1991).

Acknowledgements

We thank L. Aiello, E. Delson, B. Demes, J. Fleagle, F. Grine, W. Jungers, S. Larson, D. Lieberman, O. Pearson, D. Pilbeam, J. Polk, E. Sarmiento, R. Susman and B. Wood for providing valuable comments; F. Grine, L. Gordon, R. Thorington, R. Potts, A. Walker, and C. Ward for providing access to specimens in their care; and The Henry Luce Foundation.

Correspondence and requests for materials should be addressed to B.G.R. (e-mail: brich@gwu.edu)

Predictive accuracy of population viability analysis in conservation biology

Barry W. Brook*†, Julian J. O’Grady*, Andrew P. Chapman*, Mark A. Burgman‡, H. Resit Akçakaya§ & Richard Frankham*

* Key Centre for Biodiversity and Bioresources, Department of Biological Sciences, Macquarie University, New South Wales 2109, Australia

‡ Environmental Science, School of Botany, University of Melbourne, Parkville, Victoria 3052, Australia

§ Applied Biomathematics, 100 North Country Road, Setauket, New York 11733, USA

† Present address: Key Centre for Tropical Wildlife Management, Northern Territory University, Darwin, Northern Territory 0909, Australia

Population viability analysis (PVA) is widely applied in conservation biology to predict extinction risks for threatened species and to compare alternative options for their management^{1–4}. It can also be used as a basis for listing species as endangered under World Conservation Union criteria⁵. However, there is considerable scepticism regarding the predictive accuracy of PVA, mainly because of a lack of validation in real systems^{2,6–8}. Here we conducted a retrospective test of PVA based on 21 long-term ecological studies—the first comprehensive and replicated evaluation of the predictive powers of PVA. Parameters were

estimated from the first half of each data set and the second half was used to evaluate the performance of the model. Contrary to recent criticisms, we found that PVA predictions were surprisingly accurate. The risk of population decline closely matched observed outcomes, there was no significant bias, and population size projections did not differ significantly from reality. Furthermore, the predictions of the five PVA software packages were highly concordant. We conclude that PVA is a valid and sufficiently accurate tool for categorizing and managing endangered species.

PVA is a way to predict the probability of population (or species) extinction, by inputting actual life-history information and projecting it forward using stochastic computer simulation^{1–4}. PVA is commonly used in a comparative way, to evaluate the effectiveness of different management options; because of this it has been argued that PVA predictions do not need to be precise^{2,9,10}. However, there is no clear dichotomy between relative and absolute predictions—as conservation actions entail costs, management decisions are based not only on whether the proposed strategy is sufficient to achieve recovery, but also on whether the likely benefit will justify the expenditure. These considerations require PVA predictions to be quantitatively reliable. Uncertainties surrounding its predictive reliability have led to conclusions drawn from PVA being rejected in the law courts¹¹. It is therefore essential that the predictions of PVA be compared and tested^{12–14}. Here we assess the predictive accuracy of PVA, and determine whether different generic PVA computer packages differ in their predictive capabilities.

Historical data have been used to test and improve the predictions of complex climatic¹⁵, economic¹⁶, geological¹⁷ and ecological¹⁸ models. As PVA models have important stochastic components, the conclusions of past studies based on a single test^{13,19} lack power, and are prone to case-specific peculiarities²⁰. Consequently, a valid test of PVA predictions must incorporate a large number of data sets to obtain representative assessments. We conducted retrospective analyses on 21 wildlife populations—8 avian, 11 mammalian (representing 9 species), 1 reptilian and 1 piscine.

The 21 data sets used were the only long-term studies we identified that presented data of sufficient duration and quality to be suitable for retrospective testing (see Methods). Five of the most commonly applied ‘generic’ PVA packages (GAPPS, INMAT, RAMAS Metapop, RAMAS Stage and VORTEX) were used. These packages are all suitable for generic, single-population risk assessments. They offer the most realistic prospects for improving PVA as they are subject to wide scrutiny, are repeatedly used and are frequently revised and updated. All have been used in the management and conservation of endangered species. The key features and differences between the five PVA packages are given in the Supplementary Information.

To avoid circularity, the total data available for each population was split. The first half was used to develop and parameterize the models; the latter half was reserved for testing the accuracy of the PVA predictions. To ensure that the two time periods were kept completely separate, no information from the second half of the population history was used in formulating or parameterizing the

Table 1 Comparison of actual versus predicted quasi-extinction risks

	Expected number	GAPPS*	INMAT	R META	R STAGE	VORTEX
No. $N(\text{actual}) < N(Q 90\%)$	18.9	17	16	19	17	17
G-test P		0.48	0.07	0.94	0.21	0.21
No. $N(\text{actual}) < N(Q 50\%)$	10.5	11	10	8	11	8
G-test P		0.65	0.83	0.27	0.83	0.27
No. $N(\text{actual}) < N(Q 10\%)$	2.1	3	1	3	4	3
G-test P		0.48	0.38	0.54	0.21	0.54

The number of actual populations that declined below the predicted population size corresponding to quasi-extinction probabilities of 90%, 50% and 10%, for the population viability analysis software packages GAPPS, INMAT, RAMAS Metapop, RAMAS Stage and VORTEX. The sample is based on 21 retrospective studies. None of the PVA packages’ predictions differed significantly from the expected outcome based on goodness of fit (G) tests.

* GAPPS crashes at very large population sizes because of memory limitations, so the fish was not modelled with this package (expected numbers adjusted to 18, 10 and 2).